

CASE STUDY

Sedimentological studies of marine oil fields in order to reduce drilling risk and environmental pollution: a case study of South of Iran

Samira Abbasi¹, Saeid Pourmorad^{2*}, Ashutosh Mohanty³ and Shakura Jahan⁴

¹Department of Environment, Natural Resources Faculty, Khorramshahr University of Marine Science and Technology, Khorramshahr, Iran

²Institute of Surface-Earth System Science, Tianjin University, Tianjin, China

³Disaster Management and Environment Madhyanchal Professional University, Madhya Pradesh, India

⁴Department of Environmental Sciences at Louisiana State University, Baton Rouge, LA, United States

***Correspondence:**

Saeid Pourmorad,
omid2red@gmail.com

Received: 20 April 2023; **Accepted:** 13 May 2023; **Published:** 21 July 2023

Detailed studies of sedimentology and petrology of oil fields, especially oil fields located in the seas, play a very important role in reducing the risk of danger, increasing harvest, and reducing the amount of environmental pollution. The South Pars gas field in the waters of the Persian Gulf on the joint border line of Iran and Qatar and on the south coast of Iran has been used as a comprehensive model for this type of study. In these studies, the sedimentary environment and sequential stratigraphy of the Scorpion and Sarvak Formations in the South Pars gas field in wells 1 and 3 have been investigated. Microscopic studies and analysis of gamma-ray and acoustic diagrams of these formations have led to the identification of 9 facies in three facies belts related to wetland, dam, and open sea. Dam facies have been identified only in Sarvak formation. This study shows that the facies belts of the abovementioned formations in a ramp platform are also sloping. Sequence stratigraphy of Kazhdomi and Sarvak Formations in the study wells shows that Kazhdomi Formation has one sedimentary sequence (third category cycle) and Sarvak Formation has two sedimentary sequences. The lower boundaries of sequences 1 and 2 and the upper boundary of sequence 3 have type 1 (SB1) discontinuities, and the boundary between sequences 2 and 3 has type 2 (SB2) discontinuities.

Keywords: South Pars field, Sarvak formation, diagenetic studies, sequential stratigraphy, environmental pollution

Introduction

Sedimentological studies, especially petrographic studies, sedimentary facies, sequence stratigraphy, and stratigraphy of oil and gas fields, play a very important role in reducing drilling risks and pollution (1).

Environmental pollution can be significantly prevented with detailed geological studies and determination of ideal locations for drilling oil wells (2).

In fact, determining the type of formation and sedimentary characteristics of the formations being drilled plays an important role in determining the type of drilling mud and

environmental measures, including the use of oily and non-oily mud during drilling (3).

Sarvak Formation is known as a reservoir rock and Kazhdomi Formation is known as a very important source rock in most of Iran's oil fields (4, 5). Knowing the facies and sequences of these two formations along with their lateral changes in understanding them better is necessary to calculate the production and accumulation of hydrocarbons (6, 7).

In fact, careful study of these formations will lead to accurate paleogeographic reconstruction of albino-threonine and the factors affecting it. In addition, understanding the

depth of sea forward and backward in the samples taken and their sequential stratigraphy can be the main objectives of this study. In fact, in these studies, the data obtained from wells No. 1 and 3 have been used as a model for similar studies.

Geological location of the studied wells

South Pars gas field, the largest gas field in the world, is located in the Persian Gulf waters on the joint border line between Iran and Qatar, 100 km from the port of Asaluyeh, on the south coast of Iran and 105 km northeast of the Qatar Peninsula (Figure 1).

Research method

To study Sarvak and Kazhdomi Formations in wells No. 1 and 3 located in the South Pars gas field, paleolag data (gamma and sonic diagrams) as well as fossil and lithological studies on microscopic thin sections (Thinsections) have been used. In these studies, first, all the petrographic and diagenetic properties of the studied samples were identified, then with the help of these data, the diagenetic properties were analyzed, and a sedimentary model was drawn. In the end, the sequential stratigraphic studies of the studied wells have been investigated in detail.

In these studies, 232 microscopic thin sections were used to identify allocums and orthoschemes and to name carbonate rocks using Dunham's (8) classification. Also, to determine the facies and introduce the sedimentary model, Karuzi method (1989) has been used.

According to this method, the type of components of facies and their frequency were determined. The exact number of sedimentary sequences in wells 1 and 3 was determined by accurately determining the sedimentary environment and constituent facies.

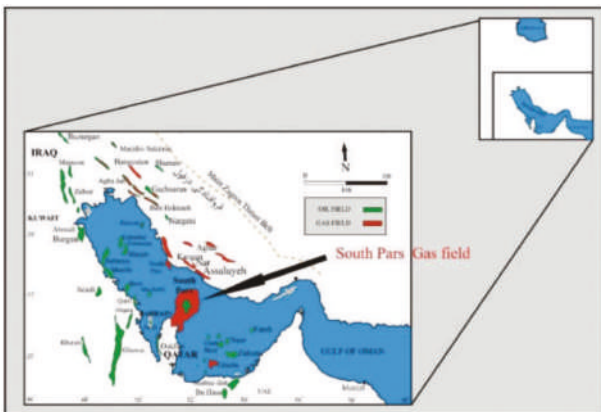


FIGURE 1 | Location of South Pars field adjacent to other oil and gas fields in the Persian Gulf and relative to the collapse of Dezful (9).

Discussion

Sarvak Formation in the sample section is 821.5 m and consists of fine-grained clay limestones and iron-bearing limestones (Figure 2) (10). This formation is divided into two members in the South Pars gas field from bottom to top based on lithological and reservoir properties: Madoud (dolomitic limestone) and Ahmadi (Chile-Marni).

Also, Ilam Formation is composed of dolomitic limestone and includes limestones of the Santonine-Campanian age (11).

Petrography of components

To identify and name microfacies and interpret the sedimentary environment, as well as to study diagenetic processes in order to interpret the diagenetic history, it is necessary to know the components in the studied samples (12).

The components in the microfacies of these two formations were classified into three groups including

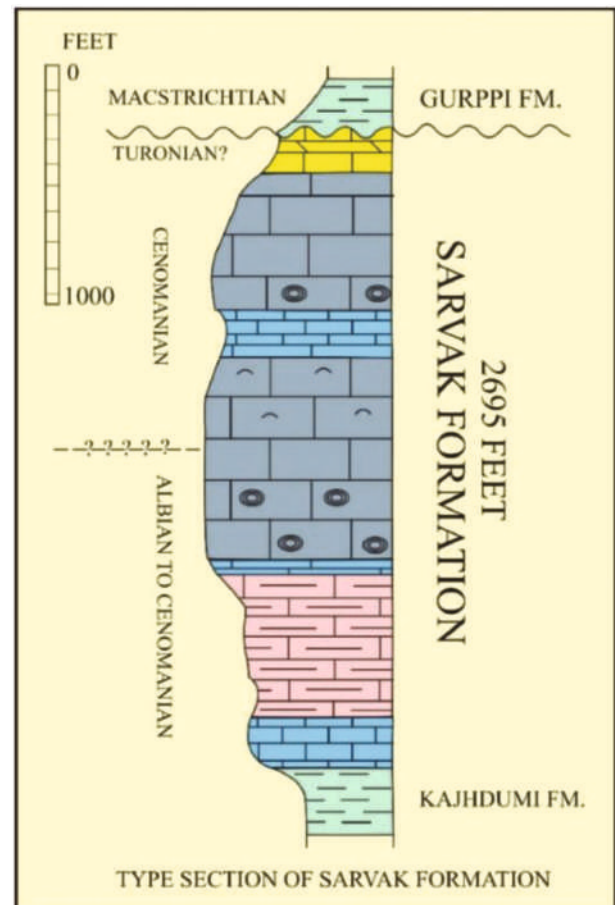


FIGURE 2 | Lithological column of Sarvak Formation in sample section in Bangestan anticline (James and wynd, 1965 with some changes).

non-skeletal carbonate components, skeletal carbonate components, and non-carbonate and detrital components.

Non-skeletal carbonate components

The most important non-skeletal carbonate components observed include proids and intraclasts. The size of peloids observed in Sarvak Formation is about 0.3–0.5 mm without internal structure. These proids make up about 30–35% of the non-skeletal carbonate components in the observed samples (**Figure 3A**). The presence of proids indicates shallow tropical and subtropical marine environments, but can also be found on continental slopes and in basins (13).

In the studied samples of Sarvak and Kazhdomi Formations in the underground sections of the South Pars gas field, intraclasts without very good sorting and in different sizes (0.3–0.7 mm) have been observed (3-B).

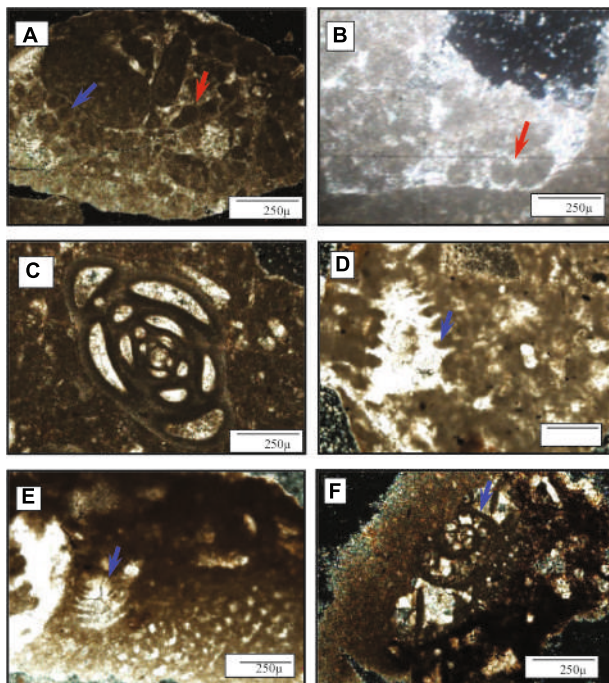


FIGURE 3 | Microscopic images of the studied samples. **(A)** Examples of proids (blue arrow) and intraclasts (red arrow) in Sarvak Formation (underground section No. SP3 of Sarvak Formation South Pars gas field, depth 1172 m, xpl light). **(B)** A sample of proids of Kozhdami Formation (underground section No. SP3 of Kozhdami Formation, South Pars gas field, depth 1245 m, xpl light). **(C)** Sample of millivolts of Sarvak Formation (underground section No. SP1 of Sarvak Formation South Pars gas field, depth 918 m, xpl light). **(D)** Trocholina altispira foraminifera in samples of Sarvak Formation (underground section No. SP3 of Kozhdami Formation of South Pars gas field, depth 1245 m, xpl light). **(E)** Benthic foraminifera Trocholina altispira in Kozhdami Formation (underground section No. SP1 Kozhdami Formation South Pars gas field, depth 1006 m, xpl light). **(F)** Hemicyclamine benthic foraminifera in Kozhdami Formation (underground section No. SP1 of Kozhdami Formation, South Pars gas field, depth 1006 m, xpl light).

Intraclasts are fragments of a loose sedimentary bed that are re-transported and deposited within the sedimentary basin (14, 15).

Skeletal carbonate components (foraminifera)

The most important carbonate components identified include Foraminifers, Ostracoda, Bivalvia, Gastropoda, Algae, Cnidaria, and Echinodermata. The most abundant foraminifera in Sarvak and Kazhdomi Formations can be of different types of miliolids (**Figure 3C**). Other foraminifera in Sarvak and Kazhdomi Formations include Orbitolina gr. concava. Miliolite and Nazaara are indicators of the swamp environment.

Orbitolina is found in the area of lagoons and dams and is in the form of wide cones that are seen in both Sarvak and Kazhdomi Formations. In the Sarvak Formation, pelagic foraminifera including lenticulina and allogesthina were also observed (**Figure 3D**). Foraminifers are composed of low or high magnesium calcite and rarely aragonite (16). Ostracodes in Sarvak and Kazhdomi Formations constitute about 5% of skeletal carbonate components. These ostriches are generally benthic and no pelagic types of ostracodes have been observed in this formation. Their average size is about 0.2 mm (**Figure 3D**).

Ostriches are valuable representations of ancient environmental conditions such as salinity, oxygen production, bed bottom, and water depth (17).

In the study areas, bivalve crust fragments with a frequency of about 5% of skeletal carbonate components have been observed. The size of these bivalves has been observed from about 0.5 mm to several millimeters. Two rudist spheres have also been observed in the Sarvak Formation (**Figures 3E, 4A**). The shell of most bivalves is composed of aragonite, and some have mixed mineralogy (18, 19).

Gastropods are one of the many components of limestone (20, 21). Gastropods are not very common in Sarvak and Kazhdomi Formations and have been seen in lagoon sections along with other fossils in the form of longitudinal and transverse sections (**Figures 5B, C**). The average size of observed gastropods has been about 0.5 mm.

Red algae are not seen in the studied underground areas and green algae are also observed to a small extent. These algae are usually located in the lagoon section (**Figure 5D**). Algae live mainly in shallow and warm environments (neritic part) of the sea and are less present in deep environments (14, 22).

Cedaria in Sarvak and Kazhdomi Formations in the studied sections form a very small part of the components (**Figure 5E**). Cedarias include anthozoans (corals) that often live in the sea and are attached to the floor (14).

Examples of this echinoderm have been observed in Sarvak and Kazhdomi Formations (**Figure 5F**). Fragments

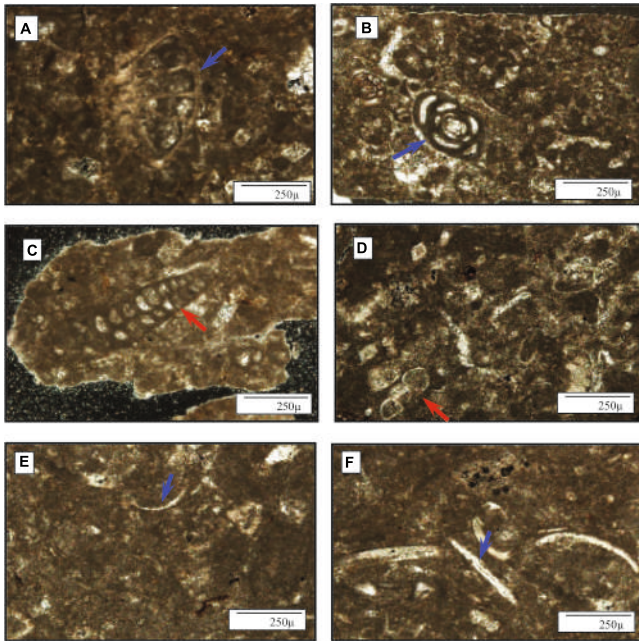


FIGURE 4 | Microscopic images of the studied samples. **(A)** A sample of Benzicene Nazazata foraminifera (underground section No. SP1 of Sarvak Formation, South Pars gas field, depth 936 m, xpl light). **(B)** An example of benthic foraminifera in Sarvak Formation. The blue arrow indicates a sample of milliolides (underground section No. SP3 of Sarvak Formation, South Pars gas field, depth 1168 m, xpl light). **(C)** Framinifer benthic textularia (underground section No. SP1 of Sarvak Formation South Pars gas field, depth 1165 m, xpl light). **(D)** A sample of pelagic foraminifera in Sarvak Formation (underground section No. SP3 of Sarvak Formation, South Pars gas field, depth of 1172 m, xpl light). **(E)** Benthic ostracod in Sarvak Formation (underground section No. SP3 of Sarvak Formation South Pars gas field, depth 1165 m, xpl light). **(F)** Fragments of two layers of Sarvak Formation (underground section No. SP3 of Sarvak Formation South Pars gas field, depth 1165 m, xpl light).

of crinoid spines have also been observed in some sections (**Figure 6A**). Echinoderm fragments are present in limestone formed in shallow marine environments plus deep marine environments (23).

Non-carbonate components

The most important non-carbonate components in the Sarvak and Kazhdomi Formations are quartz and glauconite. These components appear to be mostly of diagenetic origin (**Figures 6B, C**).

Diagenesis

The diagenesis of carbonates is associated with various processes that take place in near-sea and metallurgical environments and down to the deep burial environment (24).

The types of diagenetic processes identified in the Sarvak and Kazhdomi Formations in the South Pars gas field identified include the following:

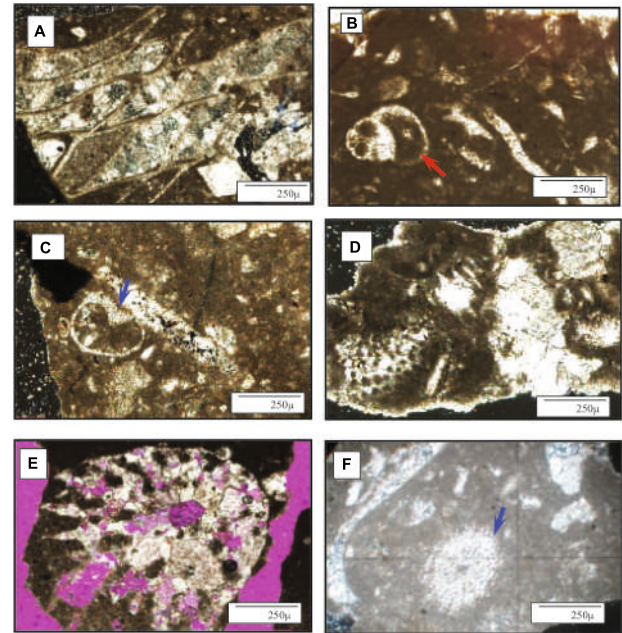


FIGURE 5 | Microscopic images of the studied samples. **(A)** A piece of two-story road in Sarvak Formation (underground section No. SP1 of Sarvak Formation South Pars gas field, depth 918 m, xpl light). **(B)** Longitudinal section of a gastropod (underground section No. SP3 No. Sarvak Formation South Pars gas field, depth 1172 m, xpl light). **(C)** Transverse section of a gastropod (underground section No. SP1 No. Kozhdami Formation of South Pars gas field, depth 1026 m, xpl light). **(D)** Green algae in samples of Sarvak Formation (underground section No. SP1 of Sarvak Formation South Pars gas field, depth 986 m, xpl light). **(E)** An example of a coral in Kozhdami Formation (underground section No. SP3 of Kozhdami Formation, South Pars gas field, depth 1212 m, xpl light). **(F)** Echinoderm section in Sarvak Formation (underground section No. SP3 of Sarvak Formation South Pars gas field, depth 1165 m, xpl light).

Cementing

In Sarvak and Kazhdomi Formations, the most important and abundant cement is calcite cement.

Cementation is a diagenetic process by which deposited minerals settle in the sediment voids and cause the sediments to become rocky Burley and Worden (25, 26).

Platy calcite cement

This cement is one of the most abundant cements in the samples and has been observed in most of the fractures and cavities in the sections and is composed of large and clear calcite crystals (**Figure 7A**).

Equant calcite mosaic cement

In the studied samples, the presence of such cements with equal crystals in the distances between the grains and also as a fracture filler has been observed (**Figure 7B**). This cement

is common in meteoric and burial diagenetic environments and is the result of a slow growth rate (27).

Drusy cement

This cement with its shaped to semi-shaped crystals in some cases has filled the inside of oysters of different organisms in the Sarvak and Kazhdomi Formations (Figures 7C, D). This cement fills some cavities, intergranular pores, and sometimes mold pores and fractures in the studied sections Bathurst (28).

Compression and compression dissolution

Compression and compression dissolution are the two main diagenetic processes that generally depend on the depth of sediment burial (29, 30). The most common structures due to compression dissolution (chemical compaction) in Sarvak and Kazhdomi Formations are stylolites (Figures 8C, D).

Neomorphism or neoplasm

The neomorphism observed in Sarvak Formation is an incremental neomorphism. In this case, dolomicrite (less than 5 microns) is converted into dolomicrospar (5–30 microns) or dolomicrospar into pseudospar (larger than 30 microns) (Figure 8E).

The phenomenon of neomorphism is associated with changes in the mineralogy or fabric of sediment (31, 32).

Dolomitization

Dolomites often form suitable hydrocarbon reservoirs because of this process, which increases porosity Allen and

Wiggins (33). Different types of dolomites in the Sarvak and Kazhdomi Formations can be determined according to the shape of the crystal border (flat or non-flat) and the size of the crystals:

Microcrystalline dolomites or dolomicrosparite

This type of dolomite is more abundant than the first type of dolomite in terms of abundance in the Sarvak and Kazhdomi Formations (Figure 9B). Dolomicrosparites are histologically the same size and their crystals are semi-shaped to shaped with planar's borders.

In this type of dolomite, the size of the crystals is 62–250 microns and they are composed of crystals of different sizes, dense, semi-shaped to amorphous, and uneven crystalline borders. These types of dolomites have a lower frequency than dolomicrosars in Sarvak Formation.

(Figure 9C) and they were not observed in the Scorpion Formation.

Ironing

Iron compounds (hematite and limonite) have been observed more abundantly in some specimens of Sarvak and Scorpion, especially in the intercrystalline pores between dolosparite crystals and dolomicrosars (Figures 10A, B). Iron compounds have also been observed along acetylides and in fossil cells (mostly foraminiferal cells). Ironmaking is generally associated with burial diagenesis.

Porosity

The types of porosities in the samples of Sarvak and Kazhdomi Formations in the South Pars gas field include the following:

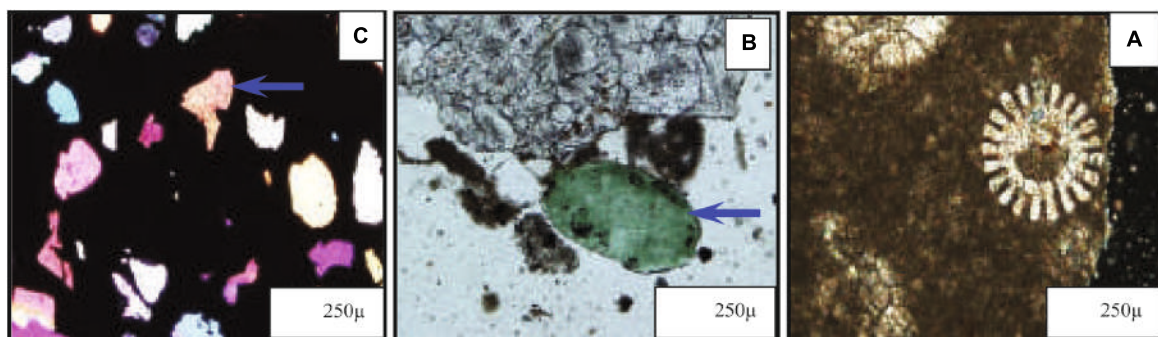


FIGURE 6 | Microscopic images of the studied samples. (A) An example of Echinoderm thorn in Sarvak Formation (underground section No. SP1 of Sarvak Formation South Pars gas field, depth 1172 m, xpl light). (B) Gluconite grain as one of the non-detrital components in Sarvak and Kozhdami Formations (underground section No. SP3 of Sarvak Formation South Pars gas field, depth 1168 m, xpl light). (C) Destructive quartz grains as non-destructive components observed in Sarvak Formation (underground section No. SP1 of Sarvak Formation South Pars gas field, depth 1172 m, xpl light).

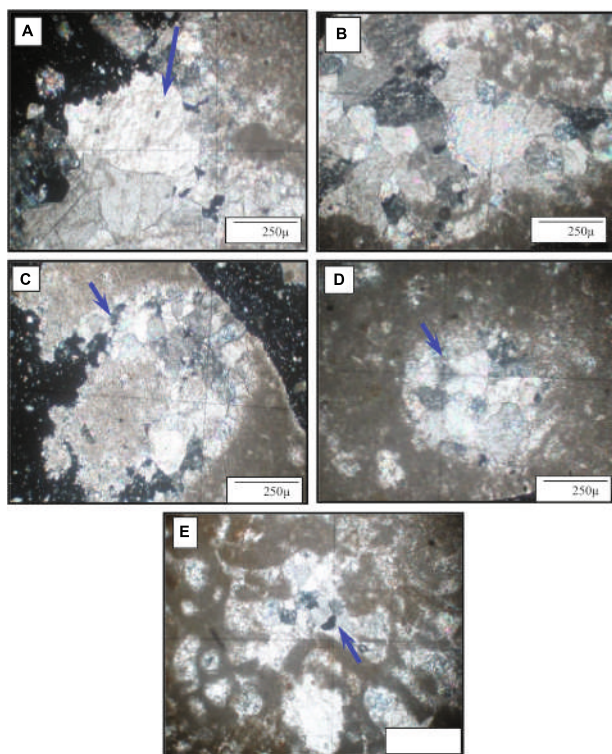


FIGURE 7 | Microscopic images of the studied samples. **(A)** Calcite plate cement—pay attention to the large crystals of this cement (underground section No. SP3 No. Kozhdami Formation of South Pars gas field, depth 1228 m, xpl light). **(B)** Calcite all-dimensional cement—pay attention to crystals approximately the same size as cement (underground section No. SP3 of Kozhdami Formation of South Pars gas field, depth 1250 m, xpl light). **(C)** Druze calcite cement—pay attention to the large crystals of this cement in the center of the hole (underground section No. SP3 No. Sarvak Formation South Pars gas field, depth 1172 m, xpl light). **(D)** Calcite Druze Cement (underground section No. SP3 of Kozhdami Formation of South Pars gas field, depth 1224 m, xpl light). **(E)** Calcite drossite cement can be seen in a cavity of Sarvak Formation. The direction of the arrow shows an increase in the size of the cement crystals (underground section number SP3 of Sarvak Formation, South Pars gas field, depth of 1165 m, xpl light).

Porosity between crystals and particles

This type of porosity is the type of primary porosity (34). This porosity is observed among dolomite crystals in Sarvak Formation, which is sometimes filled with iron oxide (Figure 10C).

Cavity porosity

In the study samples, this type of porosity, which is one of the types of secondary porosity (35), is the loss of unstable and soluble parts such as skeletal parts and shell fragments. It has created these porous pores, which are sometimes filled with anhydrite and calcite cements. This porosity is the most common type of porosity in the studied sections (Figures 10D, E, 11A).

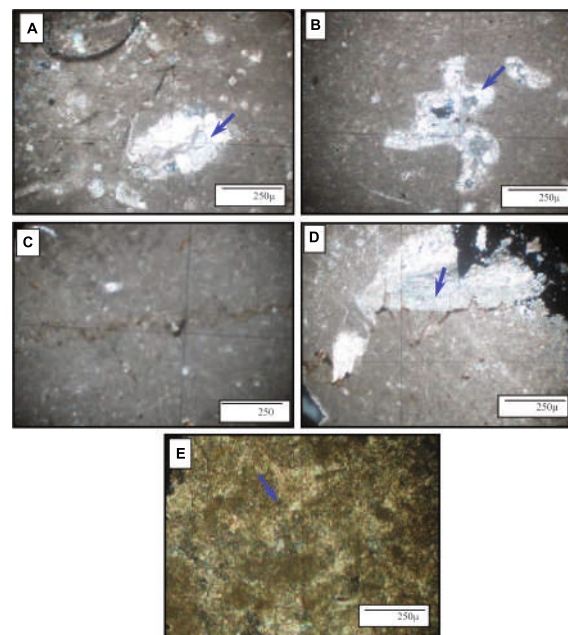


FIGURE 8 | Microscopic images of the studied samples. **(A)** Cement is also calcite dimension (blue arrow) which contains amorphous dolomite crystals (underground section No. SP3 of Sarvak Formation of South Pars gas field, depth 1172 m, xpl light). **(B)** Calcite drossite cement (blue arrow) that surrounds a hole (underground section No. SP3 of Sarvak Formation, South Pars gas field, depth 1168 m, xpl light). **(C)** Stylolite in Sarvak Formation which is filled with organic matter (underground section No. SP3 No. Sarvak Formation South Pars gas field, depth 1172 m, xpl light). **(D)** Stylolite in Kozhdami Formation which is filled with organic matter (underground section No. SP3 Kozhdami Formation South Pars gas field, depth 1245 m, xpl light). **(E)** An example of the phenomenon of neomorphism in Sarvak Formation which has caused the transformation of dolomiticite crystals into dolosparite (underground section No. SP3 of Sarvak Formation South Pars gas field, depth 1165 m, xpl light).

Moldic porosity

In the studied samples, this porosity, which is selected by the stone fabric and is secondary Bathurst (28) is mostly filled with ferrous materials or cement (Figures 10B, 11B).

Fracture porosity

Fracture porosity in carbonate rocks occurs after sediment burial (34, 36). In the studied samples, this type of porosity is observed in the fracture space along with cementation, which generally has calcite mineralogy (Figures 11B, C).

Diagenetic sequences in Sarvak and Kazhdami Formations

According to the studies, Sarvak and Kazhdami Formations have been affected by different diagenetic processes over time. Considering that the observed diagenetic processes for both formations were almost similar.

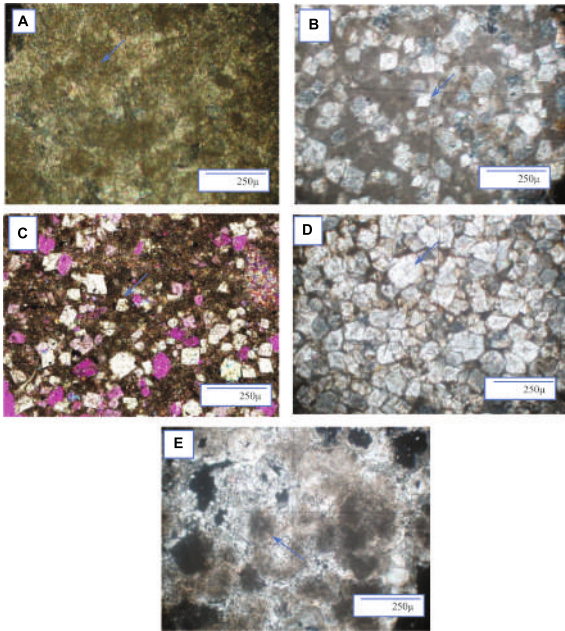


FIGURE 9 | Microscopic images of the studied samples. **(A)** Microcrystalline dolomite as one of the types of dolomites in Kozhdami Formation which is becoming coarser crystalline dolomites (underground section No. SP3 Kozhdami Formation South Pars gas field, depth 1165 m, Noor xpl). **(B)** The rhomboid crystals of dolomicrosparite in the background of the rock are known to be selectively formed (underground section No. SP3 No. Sarvak Formation South Pars gas field, depth 1165 m, xpl light). **(C)** Dolbo microsparite rhombohedral crystals in the microstatic background of Sarvak Formation (underground section No. SP3 of Sarvak Formation South Pars gas field, depth 1168 m, xpl light). **(D)** In this picture, semi-shaped crystals of dolosparite in Sarvak Formation (underground section No. SP3 of Sarvak Formation, South Pars gas field, depth 1204 m, xpl light). **(E)** Amorphous crystals of Dolosparite in samples of Sarvak Formation (underground section No. SP3 of Sarvak Formation South Pars gas field, depth 1172 m, xpl light).

Sedimentary Facies

Facies of Kazhdami Formation

Studies on the facies of this formation have led to the identification of two facies belts of wetland (A) and open sea (C).

Facies of Sarvak formation

The facies of this formation have been identified by studying microscopic samples, which has resulted in the identification of three facies belts of wetland (A), dam (B), and open sea (C) as follows:

Collection of microscopic facies of wetland environment (A)—(Lagoon facies belt)

The environment of the lagoon is limited and salinity increases due to its location behind the Reef/Greenstone dams. The diversity of organisms in this environment is low but its frequency is high (37).

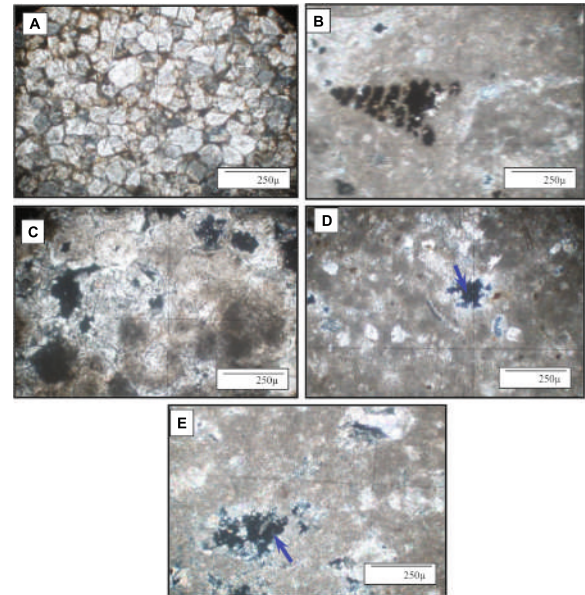


FIGURE 10 | Microscopic images of the studied samples. **(A)** Iron oxides (brown in color) and organic matter (dark in color) surround cavities, intercrystalline porosities of dolomites (underground section No. SP3, Sarvak Formation, South Pars gas field, depth 1168 m, xpl light). **(B)** Mold porosity in foraminifera filled with iron oxides (underground section No. SP3 of Sarvak Formation, South Pars gas field, depth 1204 m, xpl light). **(C)** Intercrystalline porosities in dolomites of Sarvak Formation (underground section No. SP3 of Sarvak Formation South Pars gas field, depth 1168 m, xpl light). **(D)** Pore porosity in the calcareous field of Kozhdami Formation (underground section No. SP3 Kozhdami Formation of South Pars gas field, depth 1244 m, xpl light). **(E)** Cavity porosity in Sarvak Formation (underground section No. SP3 of Sarvak Formation South Pars gas field, depth 1165 m, xpl light).

Facies A1 (Madstone/Vexton bioclast with ostracod)

This facies contains various biocells. Orbitulin and other benthic foraminifera form the most important skeletal components in this subsfacial. This facies is equivalent to the standard facies 18 for Flugel carbonate platforms (Figures 12A, B).

Facies A2 (Bioclast and Weston)

These vesicular facies contain skeletal components such as gastropods in the form of longitudinal and transverse cuts and bivalve fragments in large quantities. Other components include green algae. Diagenetic processes in this facies include advanced porosity due to fracture and cementation of skeletal components (Figure 12C).

Facies A3 (Paxton Bioclast)

The most important skeletal components of this facies include echinoderm, orbitulin, and trocholine. The amount

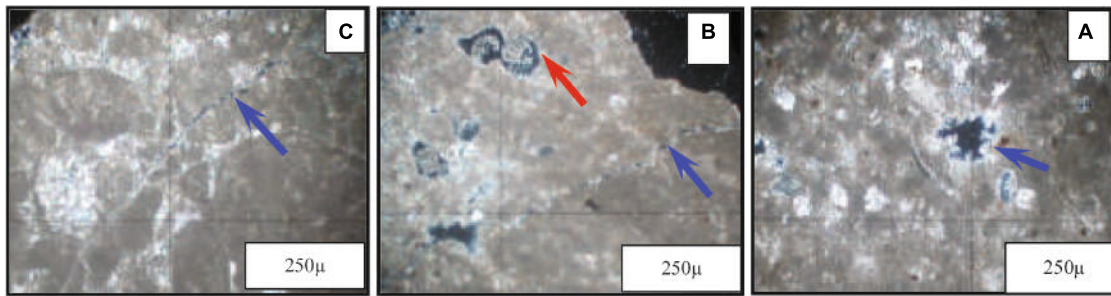


FIGURE 11 | Microscopic images of the studied samples. **(A)** In this picture, examples of cavities in the microcrystalline field in Sarvak Formation can be seen (underground section No. SP3 of Sarvak Formation, South Pars gas field, depth 1165 m, xpl light). **(B)** Porosity due to fracture (blue arrow) and mold porosity (red arrow) (underground section No. SP3 of Sarvak Formation, South Pars gas field, depth of 1165 m, xpl light). **(C)** Porosity due to fracture (blue arrow) (underground section No. SP3 No. Kozhdami Formation of South Pars gas field, depth 1208 ms, xpl light).

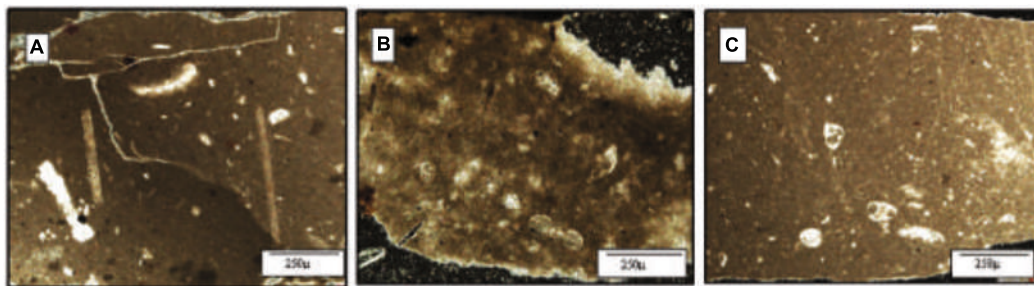


FIGURE 12 | Microscopic images of the studied samples. **(A)** Facade A1: Madstone/Westxon with extruded. It has an astra code and two cups. **(B)** Facade A1: Madstone/Waxton Bioclast. It has ostracods and bivalve crumbs. **(C)** Subfacial A2: Bioclast Westxon, bivalve, green algae gastropod.

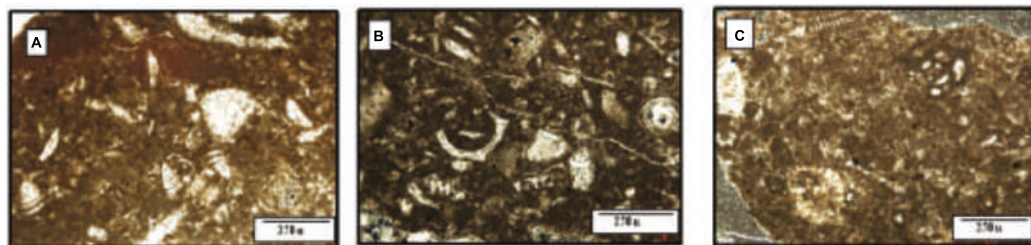


FIGURE 13 | Microscopic images of the studied samples. **(A)** Facade A3: Paxton bioclast contains trocholine, bilayer, and echinoid. **(B)**: Facade A3: BioClast Paxton contains ecoinoids, bivalves, and benthic fragments. **(C)** Facade A4: Paxton myeloid ploid contains benthic foraminifera such as myeloid and nearly matched ploid grains.

of orbitulin and trocholine reaches a maximum of 50% and echinoderm up to 20% (Figures 13A, B). This facade is equivalent to the standard Facelog No. 20 for Rug platforms (RMF20).

Facies A4 (Paxton Myeloid Ploid)

Most of this facies contains benthic foraminifera such as myeloid and almost matched ploid granules. Bifurcated fragments have also been seen in this facies. This facade is equivalent to Flogel Standard Facility No. 16 for ramp type carbonate platforms. Cementation phenomena have been observed in these facies and porosity has not been observed much in these facies (Figure 13C).

Interpretation of sedimentary environment of wetland facies belt

Group A1 and A2 facies are deposited in the low-energy part of the wetland, which mainly covers the land-facing part. Evidence of this is the presence of limestone in large quantities in its facies. In addition, the presence of skeletal components of organisms that live in the low-energy part of the lagoon, such as gastroporesis, miliolids, and green algae, is another reason for the deposition of A2 and A1 facies in the low-energy part of this environment.

The presence of ploydy in the A3 facies of this group is also important for non-skeletal granules. These non-skeletal grains are more abundant in quiet parts of the lagoon. Ploids

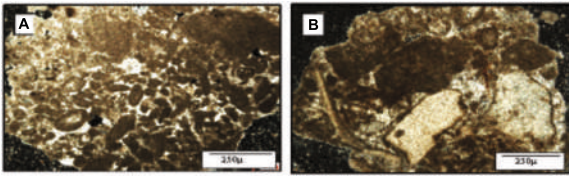


FIGURE 14 | Microscopic images of the studied samples. **(A)** Facial B1: Greenstone ploidal intracellular containing ploid and semi-matched intracellular. **(B)** Facade B2: This facade includes echinoid fragments, orbitolin foraminifera, and non-skeletal components such as intraclasts and biceps components.

are either created by organisms or created by the crushing of intercal near the dam and have entered the lagoon.

Barrier facies belt (B)

The facies belt of the dam is located between the two belts of the facies of the wetland behind the dam and the open sea and includes the following facies:

B1 loss (Ploidal intracellular greenstone)

Most of its components include ploid in the range of 50–60% and intracellular in the range of 10–15%. Ploids and intraclasts are semi-matched. This facies is equivalent to the standard microfacies No. 27 of Flugel. The phenomenon of dolomitization in this facies is sometimes observed (**Figure 14B**).

B2 facies (greenstone bioclast)

The components of this facies include echinoid fragments, orminitic foraminifera, non-skeletal components such as intraclasts, and biceps fragments (**Figure 12C**). The absence of a mud matrix indicates the energetic conditions in the deposition of this microfacies. The presence of echinoderm can indicate the part close to the open sea of the dam. This facade is equivalent to the standard 26 Flugel facies for carbonate ramp (RMF 26) platforms.

Interpretation of the sedimentary environment of the dam facies belt

Facies B1 and B2 are related to the energetic environment of the dam due to the grain size, the presence of cement, and the absence of carbonate mud.

The semicircular of the intracellular grains in the B1 facies also indicates a high-energy environment. These grains can be formed by the erosion of canal walls in a barrier medium (38). Micritic cover around skeletal grains indicates sedimentation in the area of light penetration and depth less than 100–200 m Enos (39) and Selwood (40).

Open marine facies belt

The offshore facies belt extends at the end of the carbonate platform toward the sea of dam facies/submarine hills (41). Offshore facies include the following facies.

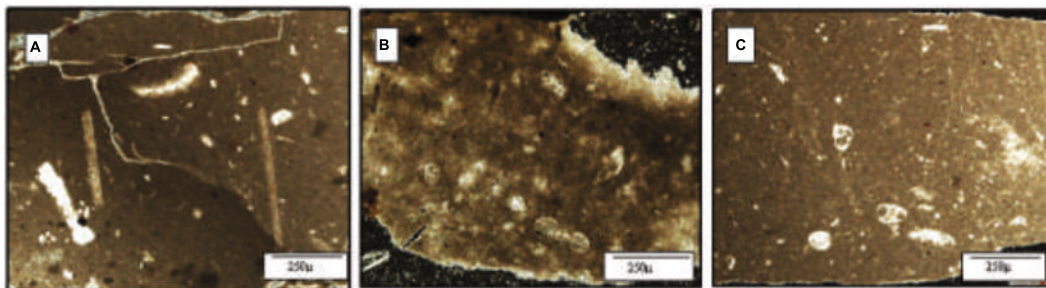


FIGURE 15 | Images of microscopic facies C1 **(A)** and C2 offshore **(B,C)**.

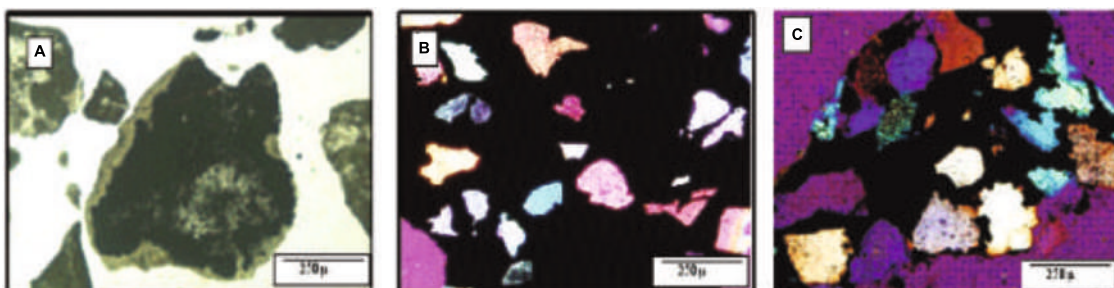


FIGURE 16 | Destructive facies in Scorpion and Sarvak structures. **(A)** Chilean facies at the base of Kazhdomi Formation, and **(B,C)**. Sandstone facies in Sarvak **(B)** and Kazhdomi **(C)** Formations.

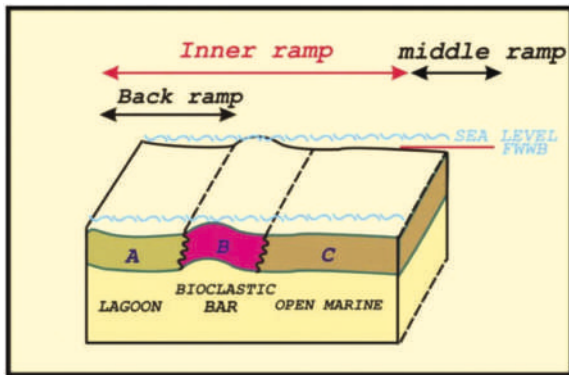


FIGURE 17 | Facies model of the studied formations, which is in accordance with the facies of a carbonate ramp, including inner and middle ramps.

Facies C1 (Madstone Bioclast): In this facies, components such as echinoderm fragments and bilayer fragments are observed. Echinoid fragments usually make up the largest number of fragments. This facade is equivalent to the standard facelifit number 9 of Flugel. This facade is related to the initial parts of the middle ramp (**Figure 15A**).

Facies C2 (vextone bioclast): This facies includes fragments of the echinoderm, sponge needle, and a limited number of pelagic foraminifera. This facade is equivalent to Standard Flogel Facility No. 5 for ramp-type carbonate platforms. These facies can be related to the end parts of the middle ramp facies (**Figures 15B, C**).

Detrital facies in Kajdomi and Sarvak Formations Shale damage

This facies is mostly observed at the base of Kazhdomi Formation. Ahmadi Shale exists as an interlayer between the limestones of this section (**Figure 14A**).

Sandstone facies

These facies have been observed sparsely in some depths of Sarvak and Kajdomi Formations (**Figures 14B, C**). Arnite quartz facies can be seen in the base parts of Kazhdomi Formation.

Interpretation of the offshore sedimentation environment C

The presence of echinoderms and spongy needles in these facies and the absence of wetland organisms such as gastropods, even in small numbers, indicate their transport to the deep parts of the open sea environment. Group C is similar to today's deep sediments of the Florida platform

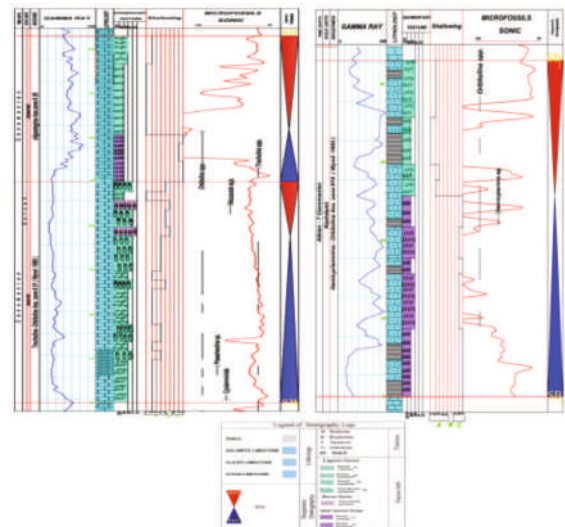


FIGURE 18 | Sequential stratigraphic column of Kazhdomi Formation in well No. 1 of South Pars gas field (top left figure) and sequential stratigraphic column of Sarvak Formation (Madoud and Ahmadi) in well No. 1 of South Pars gas field (top right figure) And finally the guide form of stratigraphic sections (bottom figure).

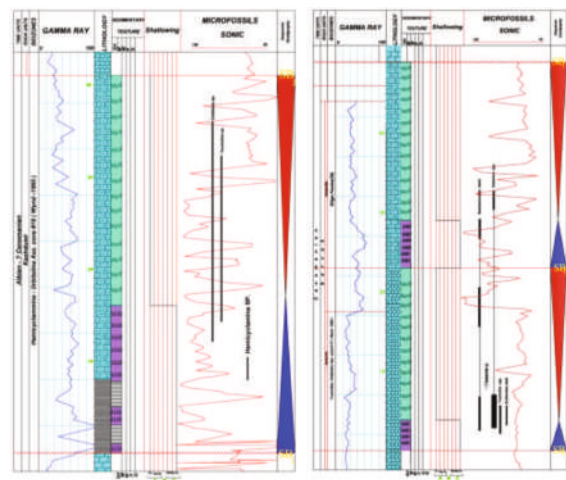


FIGURE 19 | Sequence stratigraphic column of Kozhdami Formation in well No. 3 of South Pars gas field (right figure) and sequence stratigraphic column of Sarvak Formation (Madoud and Ahmadi) in well No. 3 of South Pars gas field.

Enos (39) and Selwood (40) and the Bahamas platform Shin (42).

Sedimentary model

Based on the data obtained from the mentioned studies, calcareous facies of Kazhdomi Formation have been deposited in the above areas in the wetland and open sea environment. The facies of Sarvak Formation of well No. 3 have also been deposited in the wetland and open sea facies belt, but this formation in well No. 1 includes the wetland facies belt, dam, and open sea.

A lack of growth of dam reefs, a lack of turbidite facies, gradual changes of facies in the stratigraphic column, a lack of continuity of reef processes, and absence of aggregate grains are in accordance with a ramp-type carbonate platform (Figure 17).

Sequential stratigraphy

Sequence stratigraphy is based on the knowledge of sedimentology and stratigraphy (43, 44). In the following section, the sequential stratigraphy of the two wells studied is introduced as a model for this type of study:

According to the obtained evidence, the discontinuity of the top of the Darian Formation to the Apsin age in this region separates this formation from Kozhdi Formation of the Albin age. Sequence (I) in Kozhdi Formation is 43 m thick at the age of Albin. The time and presence of gluconite and iron oxide minerals have been determined (45, 46).

In fact, it can be said that this section was deposited as a result of the significant advance of the sea on the level of discontinuity of the Apsin end. As the sea progresses on the discontinuous surface, the TST section of this sequence is formed and includes a group of open sea facies. This part, which is 22 m thick, has a sponge needle and small amount of planktonic foraminifera. The highest MFS advanced level is located at 22 m at the base of this formation and is located between the shale layers and the open sea facies.

The HST section is 21 m thick and consists of wetland facies. *Orbitolina* has been seen in abundance in this section. *Trocholine* fossils have also been found in small amounts. The upper boundary of the sequence is due to the change of time and change of lithology of SB2 type and is located at the top of Kazhdomi Formation (Figure 16).

Sequential stratigraphy of Sarvak Formation in well No. 1 of South Pars gas field: Sequence II in this formation has a thickness of 53 m and is of Cenomanian age. The lower boundary of this sequence is of SB2 type according to the reasons mentioned above and is located at the top of Kazhdomi Formation. The TST facade handle is 38 m thick. The maximum flood level (MFS) is located at a depth of 38 m in the Madoud section.

The HST facies series includes calcareous sediments of the wetland and dam environment with a thickness of 15 m and its most important benthic foraminifera are orbitulin and trocholine. This group of facies is also located in the mud section of Sarvak Formation. The upper boundary of this sequence is SB1 due to the presence of laterite in thin sections and is located at 1 m at the base of Ahmadi Shale. Sequence 2, which is located in Ahmadi section, is 33 m thick.

The TST facies category is 11 m thick and includes the open sea facies. The maximum advanced level (MFS) in this sequence is located at 11 m at the base of Ahmadi Sarvak section and between the layers of limestone. The HST facies category is 22 m thick and includes the wetland facies. The

upper boundary of the sequence is SB1 and is located at the apex of the Ahmadi Shale and the level of the threonine discontinuity (Figure 16).

Sequential stratigraphy of Kazhdomi Formation in well No. 3 of the South Pars gas field

Kazhdomi Formation 41 in well No. 3 of South Pars is 41 m thick. Sequence 3 in Kazhdomi Formation, well No. 3, similar to this formation in well 1, is of Albin age. The SB1-type sequential boundary is located on the Darian Formation (discontinuous surface between Apsin and Albin).

Sequence I is 41 m thick. The TST facies group, which consists of offshore facies, is 16 m thick. The highest advanced level (MFS) is located between the Chilean layers and at a depth of 16 m at the base of the Scorpion. The HST facies category is 25 m thick and includes wetland facies. The upper boundary of the sequence is of type SB2 and is located between the layers of Chile Scorpion and Dolomite Modoud (Figure 17).

Sequential stratigraphy of Sarvak Formation in well No. 3 of South Pars gas field

Sequence 1, which is the age of Cenomanian, is 23 m thick. The TST facies handle is 4 m thick and includes open sea facies. The maximum advanced level (MFS) is located 4 m from the base of the head (Modoud section). The HST facies category is also located in the module section.

This category of facies is 19 m thick and includes the facies of the lagoon. *Tricholine* and *orbitulin* are abundant in these facies. The upper bound of the sequence II, as mentioned in well No. 1, is due to the presence of SB1-type laterite and is located at the base of Ahmadi Shale. Sequence 24 is 24 m thick and is located in Ahmadi Shale.

The TST facies category in this sequence is 6 m thick and includes open sea facies. *Rotalia* facies has also been "seen" in this category. The level of maximum progress in this sequence is located at a depth of 6 m at the base of the Ahmadi Shale. The HST facies handle has a thickness of 20 m, which has a wetland facade. The upper bound of sequence III is of the SB1 type due to the discontinuity between cenomanine and threonine (Figure 17).

Conclusion

The most important results of these studies, which have been used as a model for similar studies, include the following:

- Studies of Kazhdomi and Sarvak Formations have led to the identification of wetland facies belts behind the dam, dam,

and returned sea, which are divided into facies and subfacies in more detail based on their texture and components.

–Sedimentary model for Kazhdomi and Sarvak Formations located in the South Pars gas field has been determined based on the sequence of identified facies of ramp-type platform with one-way slope.

–Based on sequential stratigraphic studies of Scorpion and Sarvak structures, three third-cycle sedimentary sequences have been identified for the deposits of these two formations, including sequence I of the former Albino age, which is located in the lower and middle part of Scorpion Formation. Sequence II is of Late Albian-Early Cenomanian age, which is located from the apex of the Kazhdomi Formation to the apex of the Modoud section of the Sarvak Formation.

–The upper boundary of the Sarvak sequence is characterized by erosion discontinuities and longtime gaps. According to paleontological studies, the age of Sarvak Formation in the well (Nos. 1 and 3) is probably up to the end of Cenomanian and immediately on it; Ilam Formation is of Santonian age.

The presence of such a large discontinuity confirms the protrusion of the platform due to tectonic movements of salt (salt domes) or self-fault or activation of foundation faults.

References

- Pourmorad S, Harami RM, Solgi A. Sedimentological, geochemical and Hydrogeochemical studies of alluvial fans for mineral and environmental purposes (case study of Southwestern Iran). *Lithol Miner Resour.* (2021) 56:89–112. doi:
- Pourmorad S, Abbasi S, Patel N, Mohanty A. Investigation and potential identification of karsts as groundwater resources with the help of GIS studies, a case study of western Iran. *Lithol Min Resour.* (2022).
- Pourmorad S, Jokar A, Jahan S. Determination of key beds from the cap rocks of oil reservoirs using a novel method, case study: the Gachsaran Formation, Southwest Iran, Lithology. (2021).
- Jamalpour M, Bahauddin H, Armoon A. Lithostratigraphy and biostratigraphy of the sarvak formation in Wells No. 2, 16 and 66 of Rag-e-Safid oilfield in the Southwest of Iran. *Open J Geol.* (2017) 7:806–21.
- Yazdi-Moghadam M, Schlagintweit F. *Persiconus sarvaki* n. gen., n. sp., a new complex orbitolinid (Foraminifera) from the Cenomanian of the Sarvak Formation (SW Iran, Zagros Zone). *Cretaceous Res.* (2020) 109:104380.
- Jino Park J, Lee J, Joo Choh S. Facies analysis of the upper Ordovician Xiazhen formation, southeast China: implications for carbonate platform development in South China prior to the onset of the Hirnantian glaciation. *Facies.* (2021) 67:18.
- Sajadi S, Rashidi R. *Paleoecology and sedimentary environments of the Oligo-Miocene deposits of the Asmari Formation (Qeshm Island, SE Persian Gulf)*. London: IntechOpen (2019).
- Dunham RJ. Classification of carbonate rocks according to depositional texture. *AAPG Mem.* (1962) 1:108–21.
- Insalaco E, Virgone A, Courme B, Gaillot J, Kamali M, Moallemi A, et al. Upper Dalan member and Kangan formation between the zagros mountains and offshore Fars, Iran: depositional system, biostratigraphy and stratigraphic architecture. *GeoArabia11, Gulf PetroLink, Bahrain.* (2006):75–176.
- James G, Wynd GG. Stratigraphic nomenclature of Iranian oil consortium agreement area. *AAPG Bull.* (1965) 49:2182–245.
- Soleimani S, Aleali M. Microfacies patterns and depositional environments of the Sarvak Formation in the Abadan Plain, Southwest of Zagros, Iran. *Open J Geol.* (2016) 6:201–9.
- James N, Narbonne G, Armstrong A. Aragonite depositional facies in a Late Ordovician calcite sea. Eastern Laurentia. *Sedimentology.* (2020) 67:3513–32.
- Kroger B, Penny A, Shen Y, Munnecke A. Algae, calcitarchs and the late Ordovician Baltic limestone facies of the Baltic Basin. *Facies.* (2020) 66:12. doi: 10.1007/s10347-019-0585-0
- Flügel E. *Microfacies of Carbonate Rocks, Analysis, Interpretation and Application*. Berlin: Springer (2004). 976 p.
- Lee M, Elias R, Choh S, Lee D. Disorientation of corals in Late Ordovician lime mudstone: a case for ephemeral, biodegradable substrate? *Palaeogeogr Palaeoclimatol Palaeoecol.* (2019) 520:55–65.
- Sariaslan N, Langer M. Atypical, high-diversity assemblages of foraminifera in a mangrove estuary in northern Brazil. *Biogeogr Sci.* (2021) 18.
- Kalpana R, Saravana Bhavan P, Udayasuriyan R, Sheu J, Jayakumar T, Fong T. First record of a seed shrimp (*Ostracoda: Podocopida*) *Cypretta campechensis (Cyprididae)* in a perennial lake (Coimbatore, India): its molecular identification. *Int J Fauna Biol Stud.* (2021) 8.
- Khalil M, Ezraneti R, Rusydi R, Yasin Z, Hwai Tan S. Biometric relationship of *Tegillarca granosa (Bivalvia: Arcidae)* from the Northern Region of the Strait of Malacca. *Ocean Sci J.* (2021) 56:156–66.
- Ramesha M, Sophia S. Morphometry, length-weight relationships and condition index of *Parreysia favidens (Benson, 1862) (Bivalvia: Unionidae)* from river Seeta in the Western Ghats. *India Indian J Fish.* (2015) 62:18–24.
- Malaquias M, Stout C, Brenzinger B, Gosliner T, Valdeś A. Molecular and morphological analyses reveal pseudocryptic diversity in *Micromelo undatus (Bruguie're, 1792) (Gastropoda: Heterobranchia: Aplustridae)*. *Syst Biodivers.* (2021):1–25. doi: 10.1080/14772000.2021.1939458
- McCarthy JB, Krug PJ, Valdes A. Integrative systematics of *Placida cremoniana (Gastropoda, Heterobranchia, Sacoglossa)* reveals multiple pseudocryptic species. *Mar Biodivers.* (2019) 4.
- Ragazzola F, Kolzenburg R, Adani M, Bordone A, Cantoni C, Cerrati G, et al. Carbonate chemistry and temperature dynamics in an alga dominated habitat. *Reg Stud Mar Sci.* (2021) 44.
- Petrov N, Vladychenskaya I, Drozdov A. Molecular genetic markers of intra- and interspecific divergence within starfish and sea urchins (Echinodermata). *Biochemistry.* (2016) 81:972–80.
- Tucker ME. *Sedimentary petrology: an introduction to the origin of sedimentary rocks*. London: Blackwell, Scientific Publication (2001). 260 p.
- Burley and Worden (2004).
- Nikbakht S, Rezaee P, Moussavi-Harami R, Khanehbad M, Ghaemi F. Facies analysis, sedimentary environment and sequence stratigraphy of the Khan Formation in the Kalmard Sub-Block, Central Iran: implications for Lower Permian palaeogeography. *Neues J Geol Palaontol. Abhandlungen.* (2019) 292:129–54.
- Xie D, Yao S, Cao J, Hu W, Qin Y. Origin of calcite cements and their impact on reservoir heterogeneity in the Triassic Yanchang formation, Ordos Basin, China: a combined petrological and geochemical study. *Mar Petrol Geol.* (2020) 117:118–32. doi: 10.1016/j.marpetgeo.2020.104376
- Bathurst (1975).
- Ehrenberg S, Baek H. Deposition, diagenesis and reservoir quality of an Oligocene reefal-margin limestone succession: Asmari formation, United Arab Emirates. *Sed Geol.* (2019) 393:105535.
- Moghaddas Y, Mahari R, Shabaniyan R, Najafzadeh A. Sedimentary environment, sequence stratigraphy, diagenesis and geochemistry of the carbonate Ruteh Formation in north of Mahabad section. *J Stratigr Sedimentol Res Univer Isfahan.* (2019) 35:73–108.
- Chafeet H, Raheem M, Dahham N. Diagenesis processes impact on the carbonate Mishrif quality in Ratawi oilfield, southern Iraq. *Model Earth Syst Environ.* (2020) 6:2609–22.

32. Gharechelou S, Amini A, Bohloli B, Swennen R. Relationship between the sedimentary microfacies and geomechanical behavior of the Asmari Formation carbonates, southwestern Iran. *Mar Petrol Geol.* (2020) 116:104306.
33. Allen and Wiggins (1993).
34. Wu W, Li W. Porosity of bimodal sediment mixture with particle filling. *Int J Sediment Res.* (2017) 32:253–9.
35. Gamal H, Elkatatny S, Alsaihati A, Abdulraheem A. Intelligent prediction for rock porosity while drilling complex lithology in real time. *Comput Intell Neurosci.* (2021) 2021:12. doi: 10.1155/2021/9960478
36. Hosseini Asgarabadi Z, Khodabakhsh S, Mohseni H, Abbasi N, Halverson G, Hao Bui T. Microfacies, geochemical characters and possible mechanism of rhythmic deposition of the Pabdeh formation in SE Ilam (SW Iran). *Geopersia.* (2019) 9:89–109.
37. Sebok S, Csato I, Nemes L. Sedimentology and depositional system of a transitional shallow marine – coastal complex. Lower Visean deposits in the Central Volga-Ural Petroleum Province, Orenburg. *Central Eur Geol.* (2021) 64:113–32.
38. Tucker ME, Wright PV. *Carbonate sedimentology.* London: Blackwell, Scientific Publication (1990). 482 p.
39. Enos (1986).
40. Selwood (1996).
41. Karami S, Ahmadi V, Sarooe H, Bahrami M. Facies analysis and depositional environment of the Oligocene–Miocene Asmari Formation, in Interior Fars (Zagros Basin, Iran). *Carbonates Evaporites.* (2020) 35:118–26.
42. Shin (1986).
43. Abdalnaby W. *Structural geology and neotectonics of Iraq.* Northwest Zagros: Elsevier (2019). 320 p.
44. Moussavi-Harami R, Naseri-Karimvand F, Mahboubi A, Ghabeishavi A, Shabafrooz R. Depositional environment and sequence stratigraphy of the oligocene–Miocene deposits North and East of Dehdasht, Izeh Zone, Zagros Basin, Iran. *J Sci Islam Repub Iran.* (2019) 30:143–66.
45. Abyat Y, Abyat A, Abyat A. Microfacies and depositional environment of Asmari formation in the Zeloil oil field, Zagros basin, south-west Iran. *Carbonates Evaporites.* (2019) 34:1583–93.
46. Aiello G. Introductory chapter: an introduction to the stratigraphic setting of Paleozoic to Miocene deposits based on paleoecology, facies analysis, chemostratigraphy, and chronostratigraphy- concepts and meanings. (2019):1–14.
47. Pourmorad S, Abbasi S, Ashutosh M, Moein Z. *Geochemical and remote sensing in sedimentary mine Explorations.* Germani: Lambert publication (2022). 480 p. .
48. Pourmorad S, Ashutosh M. *Alluvial fans in Southern Iran: geological, environmental and remote sensing analyses.* Singapore: Springer Verlag (2022). 209 p. .
49. Pourmorad S, Mostofa K, Li SL, Liu CQ, Moein Z. *Drilling Engineering (Geology and Mud Engineering).* Germani: Lambert publication (2021). 480 p. .
50. Read JF. Carbonate platforms of passive (extensional) continental margins: type characteristics and evolution. *Tectonophysics.* (1982) 81:195–212.